

Simultaneous Beam and User Selection for the BeamSpace mmWave/THz Massive MIMO Downlink

Kai Wu, J. Andrew Zhang, *Senior Member, IEEE*, Xiaojing Huang, *Senior Member, IEEE*,
Y. Jay Guo, *Fellow, IEEE*, and Lajos Hanzo, *Life Fellow, IEEE*

Abstract—Beamspace millimeter-wave (mmWave) and terahertz (THz) massive MIMO constitute attractive schemes for next-generation communications, given their abundant bandwidth and high throughput. However, their user and beam selection problem has to be efficiently addressed. Inspired by this challenge, we develop low-complexity solutions explicitly. We introduce the dirty paper coding (DPC) into the joint user and beam selection problem, unveil the compelling properties of the DPC sum rate optimization in beamspace massive MIMO and exploit them for substantially simplifying the problem. We also develop three algorithms for solving the simplified problem, each having its unique merits. Furthermore, we derive the sum rate bound of the algorithms and analyze their complexity. Our simulation results validate the effectiveness of the proposed design and analysis, confirming their superiority over prior solutions.

Index Terms—Multi-user MIMO communications, lens antenna array, Butler matrix, beamspace MIMO, beam selection, user selection, sum rate, DPC, zero forcing (ZF)

I. INTRODUCTION

Millimeter-wave (mmWave) and terahertz (THz) massive MIMO communications are expected to become a reality in the next-generation era [1]–[3]. Hybrid antenna arrays constitute a key ingredient of mmWave/THz massive MIMO systems. Among other popular types, the passive multi-beam antenna array concept has attracted extensive attention due to its appealingly low power consumption in passive beamforming [4]–[6]. Such antenna arrays can be realized with the aid of circuit-type beamforming networks or quasi-optical lens [7]–[9]. Either way, the analog beamforming part often relies on multiple beams. The so-called beamspace massive MIMO exploits these beams, since communications take place in a space spanned by the beams [10].

To compensate for the severe propagation loss experienced in the mmWave and THz frequency bands, massive MIMO antenna arrays generally have a large dimension, leading to a large number of beams [11]–[13]. Restricted by factors such as power consumption and the form factor, the number of radio frequency (RF) chains is usually much smaller than that of the beams. Hence, how to select a subset of beams for best performance is a key problem in beamspace massive MIMO.

The seminal beam selection work [10] opts for the specific beams bearing the strongest channel power for each user. The method is appealingly simple but may suffer from inter-user interference. An interference-aware method is proposed in [14], which assigns a beam to a user, if only that user achieves the strongest channel power in the beam. We refer to it as *the strongest beam* of the user for convenience. For users sharing strongest beams with others, an incremental beam search is developed in [14], iteratively searching for the specific beam to maximizing the sum rate in combination with previously selected beams. The zero-forcing transmit precoding (ZF-TPC) is used for deriving the sum rate [14].

By employing ZF, incremental and also decremental beam search (removing a beam in each iteration to minimize sum rate loss) methods are developed in [15]. A two-stage beam selection scheme is designed in [16]. Using ZF, a sum rate lower bound is derived and used for formulating a convex problem for the initial beam selection. Then, an iterative algorithm is designed for refining the selection results. As a further development, the dirty paper coding (DPC) is first introduced to the beam selection problem in [17], where a decremental beam selection method is developed. The complexity of the above methods is further reduced in [18] using innovative matrix manipulations.

While the contributions reviewed above mainly consider the beam selection problem, the importance of user selection for beamspace massive MIMO is highlighted in [19]. Indeed, user selection (scheduling) has become indispensable in contemporary mobile communications networks, e.g., LTE and 5G [20]. The authors of [19] first find the best matching user subset for a candidate beam subset and then search for the user subset for maximizing the ZF sum rate. However, given M RF chains, K users and N beams, the authors assume that the optimal number of users/beams may range from one to M , hence the total number of combinations of user/beam subsets may become excessive, given by $\sum_{m=1}^M \binom{K}{m} \times \binom{N}{m}$. This may become unrealistic for real-time communications.

Hence, we are inspired to substantially reduce the complexity of user and beam selection for beamspace massive MIMO systems. To do so, we introduce DPC into our joint selection problem, going way beyond the prior art of using ZF. We first unveil the appealing properties of the DPC-based sum rate and then exploit them for drastically simplifying the joint user and beam selection problem. Three algorithms are developed for solving this challenging problem. Their performance and complexity are also analyzed. Our main contributions are summarized as follows.

- 1) We show the monotonic evolution of the DPC sum rate vs

This work is partially supported by the Australian Research Council under the Discovery Project Grant DP210101411.

K. Wu, J. A. Zhang, X. Huang and Y. J. Guo are with the Global Big Data Technologies Centre, University of Technology Sydney, Sydney, NSW 2007, Australia (e-mail: kai.wu@uts.edu.au; andrew.zhang@uts.edu.au; xiaojing.huang@uts.edu.au; jay.guo@uts.edu.au).

L. Hanzo is with the Department of Electronics and Computer Science, University of Southampton, Southampton SO17 1BJ, UK (e-mail: lh@ecs.soton.ac.uk).

the numbers of selected users and beams. We prove that selecting the same numbers of users and beams as RF chains is a sufficient condition for maximizing the DPC sum rate. This substantially reduces the number of subsets of users/beams to be probed, as compared to the prior art [19]. Using the example mentioned earlier, this number is reduced from $\sum_{m=1}^M \binom{K}{m} \times \binom{N}{m}$ [19] to $\binom{K}{M} \times \binom{N}{M}$.

- 2) We develop three attractive algorithms to solve the simplified user and beam selection problem. While the first algorithm sequentially selects users first and then beams, the second and third algorithms select users and beams simultaneously. An incremental greedy searching is employed in the algorithms. In contrast to previous user/beam selection solutions, the null projection technique is applied, in line with DPC, for iteratively maximizing the sum-rate.
- 3) We derive the sum-rate upper bound for the proposed algorithms. We also analyze their computational complexity, in comparison to previous methods. Interestingly, the proposed user and beam selection algorithms have an even lower complexity than the sole beam selection method (also using DPC) [17], yet their sum rate performance is almost the same. Simulation results are provided for characterizing the proposed algorithms and analysis.

Section II establishes the signal model and formulates the joint user and beam selection problem. Section III analyzes the DPC sum rate properties mentioned above and simplifies the joint selection problem. Section IV develops three algorithms for solving the simplified problem, followed by performance-vs-complexity analysis in Section V. Our simulation results are provided in Section VI, and we conclude the paper in Section VII.

Throughout the paper, the following notations/symbols are used, unless specified otherwise. Bold upper-case letters are used for matrices; bold lower-case for vectors; calligraphic upper-case letters, e.g., \mathcal{I} , for sets. $(\cdot)^T$ denotes transpose; $(\cdot)^H$ for conjugate transpose. $\text{diag}\{\cdots\}$ generates a diagonal matrix with the enclosed values put on the diagonal; \mathbf{I}_x denotes an x -dimensional identity matrix; $\det\{\cdot\}$ represents the matrix determinant; $\mathbb{E}\{\cdot\}$ is the expectation; \mathbb{B} denotes the set of Boolean numbers; \mathbb{C} is the set of complex numbers; \mathbb{R} is the set of real numbers; $[\mathbf{x}]_n$ denotes the n -th entry of a vector \mathbf{x} ; $[\mathbf{X}]_{a,b}$ is the (a,b) -th entry of the matrix \mathbf{X} ; $[\mathbf{X}]_{a,:}$ is the a -th row; $[\mathbf{X}]_{:,b}$ is the b -th column; $[\mathbf{X}]_{a,\mathcal{I}}$ is the a -th row with the column entries indexed by elements in the set \mathcal{I} ; $[\mathbf{X}]_{\mathcal{I},:}$ represents the rows indexed by elements in \mathcal{I} , while $[\mathbf{X}]_{:, \mathcal{I}}$ represents the columns.

II. SIGNAL MODEL AND PROBLEM FORMULATION

Let us consider the beamspace mmWave/THz massive MIMO downlink relying on a multi-antenna transmitter and single-antenna users. The transmitter is equipped with a passive multi-beam antenna array, which performs analog DFT aided beamforming [21]. Such an antenna array can be implemented using quasi-optical lens or beamforming network circuit, e.g., Butler matrix [8], [9]. In massive MIMO communications, the number N of DFT beams can be much larger

than the number M of RF chains. Moreover, we consider the typical scenario of $K(\gg M)$ users. As in previous seminal beam/user selection contributions [14]–[19], each RF chain selects one beam at most. *Thus, our task is to select $B(\leq M)$ out of N beams to serve $U(\leq B)$ out of K users so that the sum rate of the downlink communications described above is maximized.*

Let \mathbf{H} denote the $K \times N$ channel matrix. The k -th row, as denoted by $\mathbf{h}_k \in \mathbb{C}^{1 \times N}$, is the channel vector of the k -th user upon employing the widely used Saleh-Valenzuela model for mmWave/THz channels [22], [23], \mathbf{h}_k can be written as $\mathbf{h}_k = \sum_{l=0}^{L_k} \alpha_l \mathbf{a}^T(u_l)$, where L_k denotes the number of paths, α_l is the path gain, and $\mathbf{a}(u_l) \in \mathbb{C}^{N \times 1}$ is the steering vector. The n -th entry of $\mathbf{a}(u_l)$ can be formulated as $[\mathbf{a}(u_l)]_n = e^{jn u_l}$. Here, u_l is the spatial frequency of the l -th path. We have $u_l = \pi \sin \theta_l \in [-\pi, \pi]$ in a uniform linear array having half-wavelength antenna spacing, where $\theta_l \in [-\frac{\pi}{2}, \frac{\pi}{2}]$ denotes the spatial angle.

Again, the transmitter performs the DFT-based beamforming, which turns \mathbf{H} into $\tilde{\mathbf{H}} = \mathbf{H}\mathbf{F}$, termed as the so-called beamspace channel matrix. Here, \mathbf{F} is an N -dimensional DFT matrix. The (a,b) -th entry of the matrix is $[\mathbf{F}]_{a,b} = \frac{1}{N} e^{-j\frac{2\pi ab}{N}}$ ($a, b = 0, 1, \dots, N-1$). The coefficient $1/N$ is used for power normalization. Let $\mathbf{x} \in \mathbb{C}^{K \times 1}$ denote the communication signal vector of all users. The signals received by the selected users can be stacked into the following vector,

$$\mathbf{y} = \mathbf{U}\tilde{\mathbf{H}}\mathbf{B}\mathbf{P}\mathbf{A}\mathbf{U}\mathbf{x} + \mathbf{z}, \text{ s.t. } \tilde{\mathbf{H}} \triangleq \mathbf{H}\mathbf{F}, \quad (1)$$

where \mathbf{z} is a complex white Gaussian noise vector, and the other component matrices are described below.

- 1) $\mathbf{U} \in \mathbb{B}^{U \times K}$ is a user selection matrix, selecting U out of K users. It is a sub-matrix of \mathbf{I}_K , hence we have $\mathbf{U} \subset \mathbf{I}_K$;
- 2) $\tilde{\mathbf{H}} \in \mathbb{C}^{K \times N}$ is known at the transmitter for beam and user selection, as in previous work [14]–[19];
- 3) $\mathbf{B} \in \mathbb{B}^{N \times B}$ is a beam selection matrix, selecting $B(\leq M)$ out of N DFT beams. It is a sub-matrix of \mathbf{I}_N , indicating that a single beam is selected for each user and conversely each selected user is assigned a single beam;
- 4) $\mathbf{P} \in \mathbb{C}^{B \times U}$ is a TPC matrix used for suppressing the inter-user interference;
- 5) $\mathbf{\Lambda} = \text{diag}\{\cdots, \sqrt{\lambda_u}, \cdots\} \in \mathbb{R}^{U \times U}$ is a diagonal matrix adjusting the transmission power for each user.

Now, the beam and user selection problem can be modeled as:

$$\begin{aligned} \max_{\mathbf{U}, \mathbf{B}, \mathbf{U}, \mathbf{B}, \mathbf{\Lambda}} \mathcal{S} &\triangleq \log_2 \det \left\{ \frac{1}{\sigma_z^2} \mathbb{E} \{ \mathbf{y} \mathbf{y}^H \} \right\} \\ \text{s.t. } \|\mathbf{B}\mathbf{P}\mathbf{A}\mathbf{U}\mathbf{x}\|_2^2 &\leq P, \\ \mathbf{U}(\in \mathbb{B}^{U \times K}) &\subset \mathbf{I}_K, \quad 1 \leq U \leq B \leq M \ll K, \\ \mathbf{B}(\in \mathbb{B}^{N \times B}) &\subset \mathbf{I}_N, \quad 1 \leq B \leq M \ll N, \end{aligned} \quad (2)$$

where the objective function is the sum rate, and P denotes the overall transmission power.

Optimally solving the problem is difficult, not only due to the non-convex constraints but also owing to the enormous size of the feasible region. Moreover, the specific expression of \mathcal{S} varies with the choice of TPC methods. When using

the dirty paper coding (DPC) and ZF, the beam selection performance has been observed [17], [18]. For joint beam and user selection, only ZF has been considered so far [19]. In this work, we explore the application of DPC. Although DPC is computationally more complex than ZF, we will show that DPC can substantially simplify Problem (2).

III. SIMPLIFYING THE BEAM AND USER SELECTION

In this section, we first reveal the relationship between the sum rate achieved by DPC and the numbers of selected beams (B) and user (U). Then we exploit this relationship for substantially simplifying the beam- and user-selection problem.

DPC is performed based on the QR decomposition of the channel matrix [24]. The composite channel matrix of our system is $\mathbf{U}\tilde{\mathbf{H}}\mathbf{B}$ based on (1). Following the QR decomposition, we have

$$(\mathbf{U}\tilde{\mathbf{H}}\mathbf{B})^H = \mathbf{Q}\mathbf{R}, \text{ s.t. } \mathbf{Q}^H\mathbf{Q} = \mathbf{I}_U, \quad (3)$$

where \mathbf{R} is a $U \times U$ upper triangular matrix. Performing DPC is equivalent to setting \mathbf{P} as

$$\mathbf{P} = \mathbf{Q}(\mathbf{R}^H)^{-1}\mathbf{D}, \text{ s.t. } [\mathbf{D}]_{u,u} = r_u \triangleq [\mathbf{R}^H]_{u,u}, \quad (4)$$

where \mathbf{D} is a $U \times U$ diagonal matrix. In QR decomposition, $r_u \neq 0$ ($\forall u$) can be made positive. Moreover, $r_u = 0$ can be readily excluded in precoding. Hence, $r_u > 0$ ($\forall u$) is assumed by default hereafter.

Substituting (3) and (4) into (1) yields $\mathbf{y} = \mathbf{D}\mathbf{A}\mathbf{U}\mathbf{x}$. Then, the sum rate \mathcal{S} given in (2) becomes

$$\mathcal{S}_{\text{DPC}} = \sum_{u=0}^{U-1} \log_2 \left(1 + \frac{r_u^2 \lambda_u \sigma_s^2}{\sigma_z^2} \right) \stackrel{\sigma_s^2=1}{=} \sum_{u=0}^{U-1} \log_2 (1 + r_u^2 \lambda_u), \quad (5)$$

where $\sqrt{\lambda_u}$ is the u -th diagonal entry of $\mathbf{\Lambda}$, σ_s^2 denotes the power of the k -th ($\forall k \in [0, K-1]$) entry of \mathbf{x} (information signal vector), and σ_z^2 is the noise variance. For simplicity, we take $\sigma_s^2 = 1$, as is often the case in practice, and use the power loading factor λ_u for controlling the actual transmitted power for user u . We also take $\sigma_z^2 = 1$ hereafter (including the simulations) and adjust \mathbf{P} to set the signal-to-noise ratio (SNR).

Given any combination of feasible U, B, \mathbf{U} and \mathbf{B} , maximizing \mathcal{S}_{DPC} under the power constraint given in (2) leads to the popular water-filling solution,

$$\lambda_u = \left[\beta - \frac{1}{r_u} \right]_+, \text{ s.t. } \sum_{u=0}^{U-1} \lambda_u = P, \quad (6)$$

where $[x]_+ = \max\{x, 0\}$. Substituting (6) into (5) yields

$$\mathcal{S}_{\text{DPC}} = \sum_{u=0}^{U-1} [\log_2 (\beta r_u)]_+. \quad (7)$$

The sum rate \mathcal{S}_{DPC} is a function of U and B (as implied in r_u). Thus, if we can ascertain the monotonicity of the function vs these parameters, we can then exploit it for determining the

optimal values of U and B first. This motivates the following exploration.

For simplicity, we consider the asymptotic case relying on an adequate \mathbf{P} , so that the $[\cdot]_+$ in (6) and (7) can be removed. We note that this asymptotic condition may not be necessary for the results to be derived; however, without it, the analytical illustration may become tediously complicated.

Consider the general case of $U = U_1$ ($\forall U_1 < B$) and denote the corresponding DPC sum rate by \mathcal{S}_1 . Let furthermore $\beta = \beta_1$ be the upper limit used in the water filling; see (6). Based on (7) and given an adequate \mathbf{P} , we have $\mathcal{S}_1 = \sum_{u=0}^{U_1-1} \log_2 (\beta_1 r_u)$. Let us now include an additional user $u = U_1 + 1$. Given an adequate but fixed power budget \mathbf{P} , we have to deduct power from the previous U_1 users and assign it to the new user. Under the water filling power allocation, the upper limit β_1 has to decrease, say by δ , to cater for an extra user. Based on (6), the power taken from the previous U_1 users is given by $U_1 \delta$, while the power assigned to the new user is $\beta - \delta - \frac{1}{\gamma_{U_1+1}}$. Equating the two amounts gives $\gamma_{U_1+1} = \frac{1}{\beta - (U_1+1)\delta}$. Modifying \mathcal{S}_1 given above, the sum rate including the new user can be formulated by $\mathcal{S}_2 = \sum_{u=0}^{U_1-1} \log_2 ((\beta_1 - \delta) r_u) + \log_2 \left(\frac{(\beta_1 - \delta)}{\beta - (U_1+1)\delta} \right)$. The difference between the sum rates is

$$\mathcal{S}_2 - \mathcal{S}_1 = \log_2 \left(\frac{(\beta_1 - \delta)^{U_1+1}}{\beta - (U_1+1)\delta} \right) - \log_2 (\beta_1^{U_1}).$$

The first derivative of the difference with respect to (w.r.t.) δ is always positive. Moreover, we have $\lim_{\delta \rightarrow 0^+} \mathcal{S}_2 - \mathcal{S}_1 = 0$. Thus, $\mathcal{S}_2 - \mathcal{S}_1 > 0$ is ensured for any $\delta > 0$. The above discussions are summarized below.

Lemma 1: *Given an adequate \mathbf{P} , the DPC sum rate \mathcal{S}_{DPC} increases with the number U of selected users.*

The relationship between \mathcal{S}_{DPC} and the number of selected beams B is more subtle. To reveal it, we first provide a useful result whose proof is given in Appendix A.

Lemma 2: *The absolute product of the diagonal entries of \mathbf{R} , i.e., $\prod_{u=0}^{U-1} r_u$, is non-decreasing with B , where \mathbf{R} is the upper triangular matrix obtained in (3) and B is the number of selected beams.*

Let us denote the DPC sum rates at $B = B_1$ ($\forall B_1 < M$) and $B = B_1 + 1$ as $\mathcal{S}_1 = \sum_{u=0}^{U-1} \log_2 (\beta r_u)$ and $\mathcal{S}_2 = \sum_{u=0}^{U-1} \log_2 ((\beta + \epsilon) \tilde{r}_u)$, respectively. Note that the change of B leads to the changes in r_u and β , as reflected by \tilde{r}_u and $(\beta + \epsilon)$. Based on the water filling in (6), we have $\sum_{u=0}^{U-1} \beta - \frac{1}{r_u} = P$ and $\sum_{u=0}^{U-1} \beta + \epsilon - \frac{1}{\tilde{r}_u} = P$, which lead to $\beta = \frac{1}{U} \left(P + \sum_{u=0}^{U-1} \frac{1}{r_u} \right)$ and $\beta + \epsilon = \frac{1}{U} \left(P + \sum_{u=0}^{U-1} \frac{1}{\tilde{r}_u} \right)$, respectively. Substituting them back to the sum rates and after some manipulations (with details suppressed), we arrive at

$$\mathcal{S}_1 = \log_2 \left(\left(\frac{P + \sum_{u=0}^{U-1} \frac{1}{r_u}}{U} \right)^U (\prod_{u=0}^{U-1} r_u) \right);$$

$$\mathcal{S}_2 = \log_2 \left(\left(\frac{P + \sum_{u=0}^{U-1} \frac{1}{\tilde{r}_u}}{U} \right)^U (\prod_{u=0}^{U-1} \tilde{r}_u) \right).$$

Note that \tilde{r}_u ($\forall u$) is obtained at $B_1 + 1$, which is surely larger than B_1 for r_u . Upon applying Lemma 2, we have $\Pi_{u=0}^{U-1} \tilde{r}_u \geq \Pi_{u=0}^{U-1} r_u$. In high-SNR conditions, i.e., for $r_u, \tilde{r}_u \gg 1$ ($\forall u$), we can observe that the first term within the two logarithmic functions is approximately the same. The above observation supports the following statement.

Lemma 3: *Given high SNRs, implying $r_u \gg 1$ ($\forall u$), the DPC sum rate \mathcal{S}_{DPC} is a non-decreasing function of the number of selected beams, i.e., B .*

Ensured by Lemmas 1 and 3, the DPC sum rate is a non-decreasing function of U and B ; hence, a more important and interesting insight is provided below.

Proposition 1: *For the beamspace mmWave/THz massive MIMO downlink considered, a sufficient condition for maximizing the DPC sum rate is selecting $U = M$ users and $B = M$ beams, where M is the number of RF chains.*

The results obtained above can be used for simplifying the beam and user selection problem modeled in (2). In particular, the objective function in (2) can now be replaced with the DPC sum rate \mathcal{S}_{DPC} given in (7). Enabled by Proposition 1, we can now take $U = M$ and $B = M$. Consequently, the optimization variables are reduced to \mathbf{U} and \mathbf{B} solely, since the optimal \mathbf{A} can be obtained based on the water filling given in (6). Upon exploiting all the above changes, the beam and user selection problem can be reformulated as

$$\begin{aligned} \max_{\mathbf{U}, \mathbf{B}} \quad & \mathcal{S}_{\text{DPC}} = \sum_{u=0}^{M-1} [\log_2(\beta r_u)]_+ \\ \text{s.t.} \quad & \mathbf{U} \in \mathbb{B}^{M \times K}, \mathbf{B} \in \mathbb{B}^{N \times M} \subset \mathbf{I}_N, \\ & r_u \triangleq [\mathbf{R}^H]_{u,u}, (\mathbf{U} \tilde{\mathbf{H}} \mathbf{B})^H = \mathbf{Q} \mathbf{R}, \mathbf{Q}^H \mathbf{Q} = \mathbf{I}_U, \\ & \lambda_u = \left[\beta - \frac{1}{r_u} \right]_+, \sum_{u=0}^{U-1} \lambda_u = P. \end{aligned} \quad (8)$$

We develop algorithms below for solving this substantially simplified problem.

IV. PROPOSED BEAM AND USER SELECTION

Due to its non-convex nature, solving Problem (8) is still difficult. Basically, all previous related studies [14]–[19] have turned to sub-optimal greedy search. We proceed by developing such sub-optimal solutions as well. The majority of the previous contributions only consider beam selection, i.e., solely searching for \mathbf{B} with $K = M$ and hence $\mathbf{U} = \mathbf{I}$. This suggests that, if we can first determine the optimal M users out of the K candidates, the remaining problem then solely involves the beam selection. This leads to the first algorithm presented in Section IV-A.

A. Sequential User and Beam Selection

In this algorithm, we first select the M users that maximize the DPC sum rate under the full beamspace channel (i.e., with all beams involved). We then select the M beams for maximizing the DPC sum rate for the pre-determined users, as in the sole beam selection problem. Given the beamspace

channel matrix $\tilde{\mathbf{H}}$, the first user we select only has to have the strongest channel power, since no interference emanating from other users needs to be considered yet. Thus, the first user is simply selected via

$$u^* : \arg\max_{u \in [0, K-1]} \left\| [\tilde{\mathbf{H}}]_{u,:} \right\|_2^2; \quad \mathcal{U}^* = \{u^*\}, \quad (9)$$

where \mathcal{U}^* collects the optimal users.

For the u -th ($u \geq 1$) selected user, we have to maximize the channel power and meanwhile minimize the interference arriving from the users already selected. Such a user can be selected by maximizing the power of the projection of a channel vector (under test) onto the null space of the previously selected channel vectors [25]. The null space can be constructed as

$$\mathbf{N}_{\mathcal{U}^*} = \mathbf{I}_N - \tilde{\mathbf{H}}^H (\tilde{\mathbf{H}} \tilde{\mathbf{H}}^H)^{-1} \tilde{\mathbf{H}}, \quad \text{s.t. } \tilde{\mathbf{H}} = [\tilde{\mathbf{H}}]_{\mathcal{U}^*,:}, \quad (10)$$

where $[\tilde{\mathbf{H}}]_{\mathcal{U}^*,:}$ denotes a sub-matrix formed by the rows of $\tilde{\mathbf{H}}$ indexed by the elements of the set \mathcal{U}^* . Upon employing $\mathbf{N}_{\mathcal{U}^*}$, the next optimal user can be identified as

$$u^* : \arg\max_{u \in [0, K-1] \setminus \mathcal{U}^*} \left\| [\tilde{\mathbf{H}}]_{u,:} \mathbf{N}_{\mathcal{U}^*} \right\|_2^2; \quad \mathcal{U}^* = \mathcal{U}^* \cup u^*, \quad (11)$$

where $(\cdot) \setminus (\cdot)$ returns the set difference. Performing the above maximization up to $(M-1)$ times, the M users that maximize the DPC sum rate under the full beamspace channel are identified. Thus, for the sequential beam selection, we take the following \mathbf{U} in (8), i.e.,

$$\mathbf{U} = \mathbf{U}^* = [\mathbf{I}_K]_{\mathcal{U}^*,:}. \quad (12)$$

Finding \mathbf{B} in (8) can be done by the popular incremental or decremental greedy search [15]. However, in contrast to all previous treatises [10], [14]–[19], we continue using the above null space projection technique for identifying the optimal beams. Similar to (9), the first optimal beam is identified as

$$b^* : \arg\max_{b \in [0, N-1]} \left\| [\mathbf{U}^* \tilde{\mathbf{H}}]_{:,b} \right\|_2^2; \quad \mathcal{B}^* = \{b^*\}, \quad (13)$$

where \mathcal{B}^* collects the optimal beams. Then the b -th ($b \geq 1$) beam is iteratively identified as

$$b^* : \arg\max_{b \in [0, N-1] \setminus \mathcal{B}^*} \left\| [\mathbf{U}^* \tilde{\mathbf{H}}]_{:,b}^H \mathbf{N}_{\mathcal{B}^*} \right\|_2^2; \quad \mathcal{B}^* = \mathcal{B}^* \cup b^*. \quad (14)$$

Note that $\mathbf{N}_{\mathcal{B}^*}$ is the following null space constructed before solving the above problem:

$$\mathbf{N}_{\mathcal{B}^*} = \mathbf{I}_M - \tilde{\mathbf{H}} (\tilde{\mathbf{H}}^H \tilde{\mathbf{H}})^{-1} \tilde{\mathbf{H}}^H, \quad \text{s.t. } \tilde{\mathbf{H}} = [\mathbf{U}^* \tilde{\mathbf{H}}]_{:, \mathcal{B}^*}, \quad (15)$$

where $[\mathbf{U}^* \tilde{\mathbf{H}}]_{:, \mathcal{B}^*}$ denotes a sub-matrix formed by the columns of the enclosed matrix indexed by the elements in the set \mathcal{B}^* . Upon iteratively solving (14) for up to $(M-1)$ times, the M beams that maximize the DPC sum rate with the pre-selected M users are obtained. The sequential user

Algorithm 1 Sequential User and Beam Selection

Input: Beamspace channel matrix $\tilde{\mathbf{H}}$; see (1); M (RF chain number); K (user number); N (beam number)

Output: \mathcal{U}^* and \mathcal{B}^*

User selection

- 1) Solve (9) for the initial \mathcal{U}^* ;
- 2) For $m = 1 : M - 1$, perform:
 - a) Construct the null space $\mathbf{N}_{\mathcal{U}^*}$ given in (10);
 - b) For each $u \in [0, K - 1] \setminus \mathcal{U}^*$, perform:
 - i) Calculate the projection in the objective function of (11);
 - c) Solve (11) to select a new user, and update \mathcal{U}^* ;

Beam selection

- 1) Set $\mathbf{U} = \mathbf{U}^* = [\mathbf{I}_K]_{\mathcal{U}^*}$;
 - 2) Solve (13) for the initial \mathcal{B}^* ;
 - 3) For $m = 1 : M - 1$, perform:
 - a) Construct the null space $\mathbf{N}_{\mathcal{B}^*}$ given in (15);
 - b) For each $b \in [0, N - 1] \setminus \mathcal{B}^*$, perform:
 - i) Calculate the projection in the objective function of (14);
 - c) Solve (14) to select the next beam, and update \mathcal{B}^* ;
-

and beam selection procedure illustrated above is summarized in Algorithm 1.

We note that in the joint user and beam selection, the M users that are optimal under the full channel with all beams involved may not be optimal under the partial channel associated with the selected beams. A key reason for this is that we only use M beams, one for each user, for communications. When using all beams for user selection, we also have to deal with extra interference that may not exist in communications. However, Algorithm 1 is not without merits. It actually provides a performance upper bound for the joint user and beam selection problem, as it will be illustrated in Section V. Next, we develop another algorithm, reducing the unnecessary interference we have to deal with.

B. Simultaneous User and Beam Selection

Instead of selecting users first and then beams, we propose next to select them simultaneously. In so doing, we first provide an important result, as proved in Appendix B. *For convenience, we refer to the beam corresponding to the strongest channel power of a user as its strongest beam.*

Proposition 2: *Let us represent the specific event that the strongest beams of the M (out of K) users maximizing the DPC sum rate have different indexes by \mathcal{E} . Then, the probability of \mathcal{E} tends to one, provided that*

$$M \leq \bar{M} \triangleq \left\lfloor \frac{KN}{K+N} \right\rfloor, \quad (16)$$

where $\lfloor \cdot \rfloor$ represents flooring, K is the total number of users, and N is that of the beams.

Equipped with Proposition 2, we now proceed to develop an algorithm simultaneously selecting a user and a beam under a pair of complementary cases: 1) the condition (16) is satisfied; or 2) it is not. The first step is the same in both cases, namely identifying the user and the beam having the highest channel

power:

$$\{u^*, b^*\} : \argmax_{\substack{u \in [0, K-1] \\ b \in [0, N-1]}} \left\| [\tilde{\mathbf{H}}]_{u,b} \right\|_2^2; \quad \mathcal{U}^* = \{u^*\}, \quad \mathcal{B}^* = \{b^*\}, \quad (17)$$

where $\tilde{\mathbf{H}}$ is the beamspace channel matrix given in (1). The remaining $(M - 1)$ users and $(M - 1)$ beams are selected in the ensuing $(M - 1)$ iterations; each iteration has a user and also a beam selected.

Case 1: *the condition (16) is satisfied.* To select the next user and beam, we project each candidate channel vector onto a null space spanned by the selected users and beams. Unlike in Algorithm 1, the null space is no longer constructed based on the full channel information; instead, it is constructed based on the beams already selected plus the strongest beam of the user under test. The rationale is twofold: 1) the strongest beam contributes most to the received power; 2) according to Proposition 2, the strongest beam of the next user to be selected has not yet been selected almost for sure, provided that the condition (16) holds.

For the u -th user under test, we identify its strongest beam and generate a beam index set as follows,

$$\mathcal{I} = \left\{ \mathcal{B}^*, \argmax_{b \in [0, N-1]} \left\| [\tilde{\mathbf{H}}]_{u,b} \right\|_2^2 \right\}, \quad (18)$$

where \mathcal{B}^* is the set of beams selected previously. Note that \mathcal{I} has a cardinality higher than \mathcal{U}^* by one. Next, we construct the null space of the selected users with the beams in \mathcal{I} , i.e.,

$$\mathbf{N}_{\mathcal{U}^*}^{\mathcal{I}} = \mathbf{I}_{|\mathcal{I}|} - \check{\mathbf{H}}^H (\check{\mathbf{H}} \check{\mathbf{H}}^H)^{-1} \check{\mathbf{H}}, \quad \check{\mathbf{H}} = [\tilde{\mathbf{H}}]_{\mathcal{U}^*, \mathcal{I}}. \quad (19)$$

We then project the partial beamspace channel vector of the u -th user in \mathcal{I} onto the above null space and calculate the projection power

$$\mathcal{P}_u = \left\| [\tilde{\mathbf{H}}]_{u, \mathcal{I}} \mathbf{N}_{\mathcal{U}^*}^{\mathcal{I}} \right\|_2^2, \quad \forall u \in [0, K - 1] \setminus \mathcal{U}^*. \quad (20)$$

The user and its strongest beam, leading to the highest projection power, will be selected next, i.e.,

$$\begin{aligned} \mathcal{U}^* &= \mathcal{U}^* \cup u^* \\ \mathcal{B}^* &= \mathcal{B}^* \cup b^* \quad ; \text{ s.t. } \{u^*, b^*\} : \argmax_{u \in [0, K-1] \setminus \mathcal{U}^*} \mathcal{P}_u, \end{aligned} \quad (21)$$

where b^* is the index of the strongest beam of user u^* . The simultaneous user and beam selection procedure is summarized in Algorithm 2.

Case 2: *the condition (16) is NOT satisfied.* In this case, only probing the strongest beam of each user candidate may lead to poor sum rate performance, since more than one selected users can achieve the strongest channel power in the same beam. However, according to Proposition 2, we can readily state that the first \bar{M} users to be selected will not share the strongest beams almost for sure. Consequently, to select the first \bar{M} users, we can continue solving (17) and (21). Then, for the remaining $(M - \bar{M})$ users, we have to test more than one beam for each user candidate. Since the second strongest

Algorithm 2 Simultaneous User and Beam Selection

Input: Beamspace channel matrix $\tilde{\mathbf{H}}$; see (1); N (beam number); K (user number); M (RF chain number)

Output: \mathcal{U}^* and \mathcal{B}^*

- 1) Calculate \bar{M} based on Proposition 2;
 - 2) Solve (17) for initial \mathcal{U}^* and \mathcal{B}^* ;
 - 3) For $m = 1 : \min\{M, \bar{M}\} - 1$, iteratively perform:
 - a) For each $u \in [0, K-1] \setminus \mathcal{U}^*$, perform:
 - i) Construct the beam index set \mathcal{I} as per (18);
 - ii) Construct the null space $\mathbf{N}_{\mathcal{U}^*}^{\mathcal{I}}$ as per (19);
 - iii) Calculate the projection \mathcal{P}_u given in (20);
 - b) Solve (21) for the next user and beam; update \mathcal{U}^* and \mathcal{B}^* ;
 - 4) If $M > \bar{M}$, proceed; otherwise, terminate.
 - 5) For $m = \bar{M} : M - 1$, iteratively perform:
 - a) For each $u \in [0, K-1] \setminus \mathcal{U}^*$ and each $i = \{0, \pm 1\}$, perform:
 - i) Construct the beam index set $\tilde{\mathcal{I}}^i$ as per (22);
 - ii) Calculate the projection $\tilde{\mathcal{P}}_u^i$ given in (23);
 - b) Solve (24) for the next user and beam; update \mathcal{U}^* and \mathcal{B}^* ;
-

beam can only be one of the neighbors in the vicinity of the strongest beam, we propose to test the three beams¹.

Based on \mathcal{I} given in (18), we construct the following three beam sets, as differentiated by the superscript,

$$\begin{aligned} \tilde{\mathcal{I}}^i &= \{\mathcal{B}^*, \langle b^* + i \rangle_N\}, \quad i = \{0, \pm 1\}, \\ \text{s.t. } b^* &: \arg\max_{b \in [0, N-1]} \left\| \left[\tilde{\mathbf{H}} \right]_{u, b} \right\|_2^2, \end{aligned} \quad (22)$$

where $\langle x \rangle_N$ denotes the modulo- N of x . For each beam set, we can construct a null space as done in (19). Then, we can project the partial beamspace channel vector of the user under test onto the null space, and calculate the projection power. The above three steps can be jointly described by

$$\begin{aligned} \tilde{\mathcal{P}}_u^i &= \left\| \left[\tilde{\mathbf{H}} \right]_{u, \tilde{\mathcal{I}}^i} \mathbf{N}_{\mathcal{U}^*}^{\tilde{\mathcal{I}}^i} \right\|_2^2, \quad i = \{0, \pm 1\}; \\ \text{s.t. } \mathbf{N}_{\mathcal{U}^*}^{\tilde{\mathcal{I}}^i} &= \mathbf{I}_{|\tilde{\mathcal{I}}^i|} - \tilde{\mathbf{H}}^H (\tilde{\mathbf{H}} \tilde{\mathbf{H}}^H)^{-1} \tilde{\mathbf{H}}, \quad \tilde{\mathbf{H}} = \left[\tilde{\mathbf{H}} \right]_{\mathcal{U}^*, \tilde{\mathcal{I}}^i}. \end{aligned} \quad (23)$$

The user and beam, leading to the highest projection power, will be selected next, i.e.,

$$\begin{aligned} \mathcal{U}^* &= \mathcal{U}^* \cup u^*; \quad \mathcal{B}^* = \mathcal{B}^* \cup b^* + i^*, \\ \text{s.t. } \{u^*, i^*\} &: \arg\max_{\substack{u \in [0, K-1] \setminus \mathcal{U}^* \\ i \in \{0, \pm 1\}}} \tilde{\mathcal{P}}_u^i; \quad b^* \text{ in (22)}. \end{aligned} \quad (24)$$

Again, Algorithm 2 summarizes the two cases for the proposed simultaneous user and beam selection. The \bar{M} derived in Proposition 2 is used as a threshold, so that we can proceed up to Step 4) if $M \leq \bar{M}$ or proceed further if the condition does not hold. Next, we provide a variant of Algorithm 2 having a lower complexity and a slight performance loss. However, the asymptotic sum rate performance of the next algorithm is the same as Algorithm 2, as it will be seen shortly.

¹More beams can be tested, but this results in negligible performance difference, as will be validated by Fig. 5 in Section VI.

Algorithm 3 Simultaneous User and Beam Selection with Lower Complexity

While sharing most of Algorithm 2,

1. Replace \mathcal{P}_u in Step 3)-a)-iii) with γ_u^i ($i = 0$) in (25);
 2. Replace $\tilde{\mathcal{P}}_u^i$ in Step 5)-a)-ii) with γ_u^i ($i = 0, \pm 1$) in (25).
-

C. Low-Complexity Simultaneous User and Beam Selection

Algorithms 1 and 2 employ null space projection to search for the optimal beams and/or users in each iteration. However, the construction of null spaces can be computationally heavy. The reason for using the null space projection is to look for the next user (beam) that suffers from the minimum interference inflicted by the previous users (beams). In the mmWave/THz massive MIMO system considered, the null space projection can be approximated by matrix multiplications, thanks to the following result.

Corollary 1: *The strongest channel components of the M selected users are asymptotically orthogonal, given a sufficiently large K and N .*

Proof: Given $K \gg M$, Proposition 2 suggests that the strongest beams of the M selected user are different with the probability approaching one. On the other hand, the channel components underlain by the strongest beams are asymptotically orthogonal as N increases [22, Lemma 1]. ■

Corollary 1 further suggests that the rows of $\tilde{\mathbf{H}}$ can be approximately orthogonal. Thus, we can suppress the null space projection and turn to our conventional but effective metric, namely the signal-to-interference ratio (SIR). Referring to (23), $\left[\tilde{\mathbf{H}} \right]_{u, \tilde{\mathcal{I}}^i}$ is the channel vector of the user under test, and $\tilde{\mathbf{H}}$ is the channel matrix of selected users. The signal power is the power in $\left[\tilde{\mathbf{H}} \right]_{u, \tilde{\mathcal{I}}^i}$, while the interference power can be obtained from the inner product between $\left[\tilde{\mathbf{H}} \right]_{u, \tilde{\mathcal{I}}^i}$ and $\tilde{\mathbf{H}}$. Thus, we can define the following SIR,

$$\gamma_u^i \approx \left\| \left[\tilde{\mathbf{H}} \right]_{u, \tilde{\mathcal{I}}^i} \right\|_2^2 / \left\| \left[\tilde{\mathbf{H}} \right]_{u, \tilde{\mathcal{I}}^i} \tilde{\mathbf{H}}^H \right\|_2^2. \quad (25)$$

The beam and user selection procedure using (25) is summarized in Algorithm 3.

V. PERFORMANCE AND COMPLEXITY ANALYSIS

We analyze the sum rate performance first and then the computational complexity of the proposed user and beam selection algorithms.

A. Performance Analysis

Corollary 2: *The upper bound of the sum rate attained by Algorithms 1-3 can be expressed as*

$$\bar{S} = S_{\text{DPC}}|_{\mathbf{U}=\mathbf{U}^*, \mathbf{B}=\mathbf{I}_N}, \quad (26)$$

where the right-hand side is obtained by substituting the variable values in the subscript into (8), and \mathbf{U}^* is given in (12).

Proof: Since \mathbf{B} is the beam selection matrix, taking $\mathbf{B} = \mathbf{I}_N$ means that all beams are used for calculating the sum rate,

i.e., without beam selection. Note that $\mathbf{B} = \mathbf{I}_N$ is feasible for the sum rate computation in (8), but it is infeasible practically, since it has the same number of columns as RF chains.

Upon applying Lemma 3, we have that $\mathbf{B} = \mathbf{I}_N$ is a sufficient condition for maximizing the DPC sum rate, given $\mathbf{U} = \mathbf{U}^*$. As given in (12), \mathbf{U}^* is constructed based on the optimal \mathcal{U}^* obtained by the first part, up to Step 2c), of Algorithm 1. All three algorithms use the incremental user selection. Thus, we can state that \mathcal{U}^* obtained by the first part of Algorithm 1 leads to the maximum sum rate, since it is the only one employing the full channel information. ■

Corollary 3: For $K = M$, Algorithm 2 achieves a sum rate upper bounded by Algorithm 1.

Proof: The condition of $K = M$ indicates that no user selection is necessary. In other words, Algorithms 1 and 2 return the same set of selected users.

Both algorithms use the incremental greedy beam selection. However, Algorithm 1 always involves all users in each iteration, while Algorithm 2 does not. Moreover, according to Lemma 1, we know that the sum rate is an increasing function of the number of users. ■

Remark 1: For $K = M$, the sum rate of Algorithm 2 can be close to that of Algorithm 1. This is mainly due to the threshold \bar{M} derived in Proposition 2. This allows us to achieve approximate optimality for the first \bar{M} selected users, since their strongest channel components are nearly orthogonal, according to Corollary 1. The threshold \bar{M} also allows us to probe extra beams for the remaining $(M - \bar{M})$ users, hence substantially reducing sum rate loss.

Remark 2: For $K \gg M$ and large N , Algorithm 2 generally achieves a higher sum rate than Algorithm 1. The condition $K \gg M$ implies that we can almost always find M users having different strongest beams. Then, Corollary 1 indicates that these users have nearly orthogonal strongest channel components. Thus, the simultaneous user and beam selection approximately minimizes the interference in each iteration. By contrast, Algorithm 1, using the full channel information, has to deal with extra interference during the user selection.

B. Computational Complexity

1) *User Selection in Algorithm 1:* Step 1) has a complexity order of $\mathcal{O}(KN)$. Step 2a) has a complexity order $\mathcal{O}(m^2)$, which only accounts for computing $(\check{\mathbf{H}}\check{\mathbf{H}}^H)^{-1}$ in the null space. The other matrix multiplication will be jointly evaluated with Step 2b-i). Note that the direct computation of the inverse has a complexity of $\mathcal{O}(m^3)$, but here we employ the iterative update of the matrix inverse [25]. Based on (10) and (11), the complexity of Step 2b-i) is given by $\mathcal{O}(N + Nm + m^2 + m)$, where m is the cardinality of \mathcal{U}^* in the m -th iteration and the norm in (14) is computed via $\left\| \begin{bmatrix} \check{\mathbf{H}} \\ \mathbf{N}_{\mathcal{U}^*} \end{bmatrix} \right\|_2^2 = \begin{bmatrix} \check{\mathbf{H}} \\ \mathbf{N}_{\mathcal{U}^*} \end{bmatrix}^H \begin{bmatrix} \check{\mathbf{H}} \\ \mathbf{N}_{\mathcal{U}^*} \end{bmatrix}$. According to Step 2b), Step 2b-i) is performed $(K - m)$ times in the m -th ($m \in [1, M - 1]$) iteration. To sum up, the overall complexity

of the user selection is

$$\sum_{m=1}^{M-1} \mathcal{O}[(K - m)(N + Nm + m^2 + m)] + \mathcal{O}(m^2) + \mathcal{O}(KN) \stackrel{N \gg M; K \gg M}{\approx} \mathcal{O}(KM^2N). \quad (27)$$

2) *Beam Selection in Algorithm 1:* Step 2) has a complexity of $\mathcal{O}(MN)$. Step 3a) has a complexity of $\mathcal{O}(m^2)$, which only accounts for computing $(\check{\mathbf{H}}^H\check{\mathbf{H}})^{-1}$ in the null space. The other matrix multiplication will be jointly evaluated with Step 3b-i). Based on (14) and (15), the complexity of Step 3b-i) is given by $\mathcal{O}(M + Mm + m^2 + m)$, where m is also the cardinality of \mathcal{B}^* in the m -th iteration. According to Step 3b), Step 3b-i) is performed for up to $(N - m)$ times in the m -th ($m \in [1, M - 1]$) iteration. To sum up, the overall complexity of the beam selection is

$$\sum_{m=1}^{M-1} \mathcal{O}[(N - m)(M + Mm + m^2 + m)] + \mathcal{O}(m^2) + \mathcal{O}(MN) \stackrel{N \gg M}{\approx} \mathcal{O}(M^3N). \quad (28)$$

The complexity is unrelated to K now, since the beam selection in Algorithm 1 is based on the M selected users.

3) *Algorithm 2:* We only illustrate the case of $K \gg M$ for brevity. In this case, the algorithm runs up to Step 4). Step 2) has a complexity of $\mathcal{O}(KN)$. Step 3a-i) can share the intermediate results of Step 2) and hence does not incur any extra complexity. Step 3a-ii) has a complexity of $\mathcal{O}(m^2)$, which again only accounts for computing $(\check{\mathbf{H}}^H\check{\mathbf{H}})^{-1}$ in the null space. Step 3a-iii) has a complexity of $\mathcal{O}[(m + 1) + (m + 1)m + m^2 + m]$, where $(m + 1)$ is the size of \mathcal{I} and m is the size of \mathcal{U}^* ; see (20). As per Step 3a), Step 3a-ii) and Step 3a-iii) are performed $(K - m)$ times for the m -th ($m \in [1, M - 1]$) iteration. In a nutshell, the overall complexity is

$$\sum_{m=1}^{M-1} \mathcal{O}[(K - m)((m + 1) + (m + 1)m + m^2 + m + m^2)] + \mathcal{O}(KN) \stackrel{K \gg M}{\approx} \mathcal{O}(KM^3). \quad (29)$$

4) *Algorithm 3:* Based on (25), computing γ_u^i has a complexity of $\mathcal{O}[(m + 1) + m(m + 1) + m]$. Note that the size of $\tilde{\mathcal{I}}_u^i$ therein is $(m + 1)$, and the size of the matrix $\check{\mathbf{H}}$ is $m \times (m + 1)$. Since the matrix inversion in Step 3a-ii) is no longer necessary, the complexity of Step 3a-ii) and Step 3a-iii) becomes just $\mathcal{O}[(m + 1) + m(m + 1) + m]$. Similar to (29), the overall complexity is

$$\sum_{m=1}^{M-1} \mathcal{O}[(K - m)((m + 1) + m(m + 1) + m)] + \mathcal{O}(KN) \stackrel{K \gg M}{\approx} \mathcal{O}\left(\frac{1}{3}KM^3\right). \quad (30)$$

Strictly, the coefficient $\frac{1}{3}$ should be removed under the big-O operation, but we keep it to show that Algorithm 3 can indeed further reduce the complexity of Algorithm 2.

Remark 3: From the above analysis, we see that Algorithms 2 and 3 have substantially lower complexity than

TABLE I: Simulation Parameters

Var.	Description	Value
N	antenna/beam number	256
K	total user number	40
M	RF chain number	16
σ_z^2	noise power; see (5)	1 (0 dB)
P	transmission power in Watt	[0, 30] dB
P/σ_z^2	SNR	[0, 30] dB
-	channel path number per user	3 (one LoS and two NLoS paths)
-	channel power	0 dB for LoS; -10 dB for NLoS
-	AoD of all paths	uniform in $[-90^\circ, 90^\circ]$

Algorithm 1. Moreover, all three algorithms have much lower complexity than the state-of-the-art joint user and beam selection method of [19]. A key reason is that the properties of the DPC sum rate we have unveiled in Lemmas 1 and 3 allow us to fix the numbers of user and beams to be selected. We note that the properties unveiled for DPC sum rate in this work may not be applicable to ZF.

Remark 4: It is interesting to observe that Algorithm 2 and 3 actually have lower complexity than the sole beam selection part of Algorithm 1. The latter has a complexity resembling the existing beam selection methods of [17], [18]. This indicates that despite their reduced complexity, the proposed Algorithm 2 and 3 achieve a similar sum rate to that of the DPC-based incremental greedy beam selection schemes of [17].

VI. SIMULATION RESULTS

Simulation results are provided to validate the proposed designs, in comparison to both the performance bounds derived and to existing benchmark methods. Unless otherwise stated, the parameter settings of Table I will be used. The settings in the table are popularly used in previous user and/or beam selection studies [14], [17]–[19].

Although the most closely related work is [19] that considers joint user and beam selection, this can be unsuitable to be a benchmark. One reason for this is that DPC is used in our work, while ZF is used in [19]. Since DPC is known to outperform ZF in terms of its sum rate performance [24], we cannot claim that the performance gain arises from our user and beam selection algorithms. Moreover, as illustrated in Proposition 1, $U = M$ and $B = M$ is sufficient for maximizing the DPC sum rate, where U (B) is the number of selected users (beams). By contrast, as shown in [19], the ZF sum rate can be maximized when $U < M$. As such, it may be deemed unfair to compare the prior art [19] to our work. When the total number of users and RF chains is the same, i.e., $K = M$, the user and beam selection turns into a beam selection problem. Thus, we identify [17], [18] as benchmark methods for the case of $K = M$, since they also use DPC and perform greedy search.

Fig. 1 plots the sum rate versus SNR, where $K = 40$ is higher than the three M values employed. We see that Algorithm 2 achieves the best performance (closest to the upper bound derived in Corollary 2), Algorithm 3 is the second, and Algorithm 1 is the third. This first consolidates our motivation of developing Algorithm 2, i.e., avoiding extra interference of using the full channel information as in Algorithm 2. This also demonstrates the success of Algorithm 2 in so doing. Observed

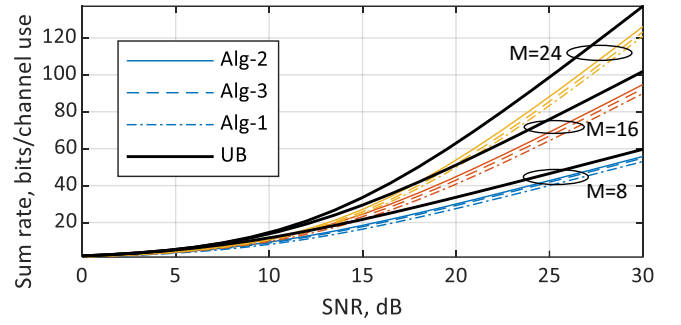


Fig. 1: Sum rate versus SNR for the case of $K > M$, where $K = 40$ in (2), UB stands for upper bound, as given in Corollary 2.

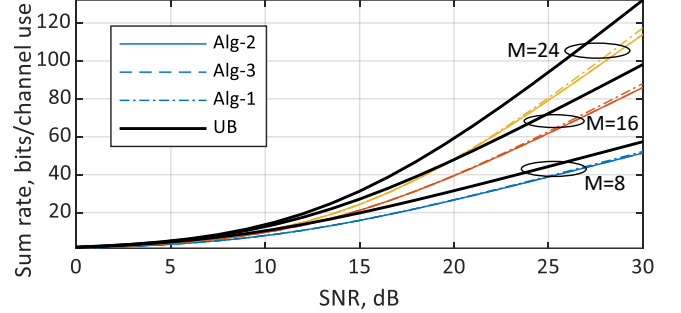


Fig. 2: Sum rate versus SNR for the case of $K = M$ in (2), where UB stands for upper bound, as given in Corollary 2. In this case, the performance of Algorithm 1 is equivalent to that of benchmark methods [17], [18].

from Fig. 1, Algorithm 3 achieves a similar performance to that of Algorithm 2. This validates the effectiveness of using the SIR to replace the null space projection, as developed in Section IV-C. Given the small performance gap and the lower complexity quantified in Section V-B, Algorithm 3 may be viewed as being more attractive than Algorithm 2.

Fig. 2 observes the sum rate versus SNR under $K = M$, where no user selection is necessary. As stated earlier, this is a sole beam selection scenario, and Algorithm 2 may be regarded as the benchmark method [17]. As indicated by Fig. 2, the three algorithms achieve similar sum rate performance, but Algorithm 1 is slightly better in the high-SNR region. This validates the result in Corollary 3. This also confirms the analysis in Remark 1. Moreover, as pointed out in Remark 4, our proposed algorithms have much lower complexity than the prior art [17]. Jointly observing Figs. 1 and 2, we can infer that the sum rate is closer to the upper bound in the case of $K > M$. Intuitively, this is because the higher the number of users, the more likely we can select a small subset of users having better angular orthogonality; see also Proposition 2 and Corollary 1.

Fig. 3 illustrates the sum rate gap versus the number of RF chains (M), where the gap is the difference between the upper bound, as given in Corollary 2, and the sum rate achieved by one of the algorithms. So the gap can be viewed as the sum rate loss. We observe that before M increases to a certain value, Algorithm 2 and 3 have lower sum rate loss than Algorithm 1. This again validates our analysis in Remark 2. We also see that, in all cases, Algorithm 2 has lower sum rate loss than Algorithm 3. This is to be expected, since Algorithm 3

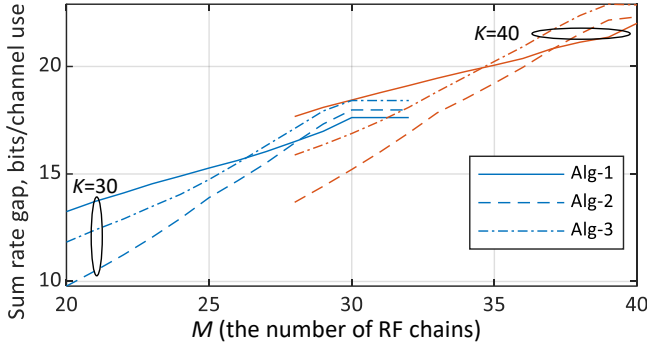


Fig. 3: Sum rate against M in (2), where the SNR is 28 dB. The gap is the difference between the upper bound and the sum rate achieved by an algorithm.

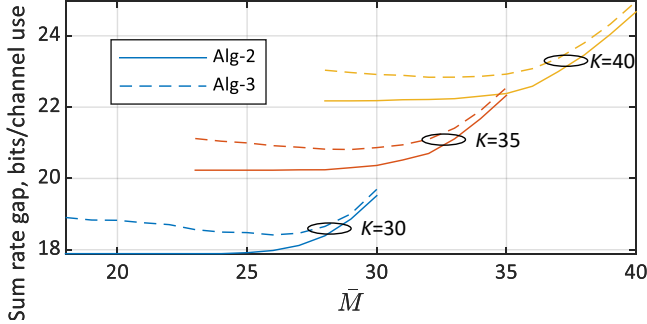


Fig. 4: Sum rate gap versus \bar{M} in (16), where $P = 28$ dB; see (8), and $M = 30, 35$ and 40 for the same values of K .

is based on an approximate orthogonality, while Algorithm 2 builds on the orthogonal null space projection. From Fig. 3 we can also see an interesting change in the performance gain of Algorithm 2/3 over that of 1. There is an intercept point, beyond which the performance gain turns from positive to negative. This corresponds to the threshold of \bar{M} , as derived in Proposition 2. However, the positive gain has a much higher value.

Fig. 4 illustrates the sum rate gap versus \bar{M} which is an intermediate variable used in Step 4) of Algorithm 2. We use Proposition 2, the upper limit of \bar{M} and $\left\lfloor \frac{KN}{K+N} \right\rfloor = 26, 30$ and 34 for $K = 30, 35$ and 40 , respectively. (Note that the corresponding upper limits of \bar{M} are used for the previous figures.) Observed from Fig. 4, the sum rate remains near-constant when \bar{M} is lower than the upper limit. However, the sum rate gap increases, as \bar{M} exceeds the upper limit. These results further confirm the validity of the analysis in Proposition 2 and the precision of the upper limit of \bar{M} derived therein. Moreover, we emphasize that the upper limit should be used whenever possible, since it minimizes the complexity of Algorithm 2 if Step 5) has to be performed.

Fig. 5 quantifies the sum rate performance versus the numbers of i values used in Step 5a) of Algorithm 2. Recall that i is the index offset introduced to help us avoid selecting the same beam as previously selected; see Section IV-B. From Fig. 5, we can only see a slight improvement as the number of i values increases from two to three. This confirms the validity of only taking three values of i , i.e., 0 and ± 1 in Algorithm 2. We underline that “three” is not a guess, the rationale has

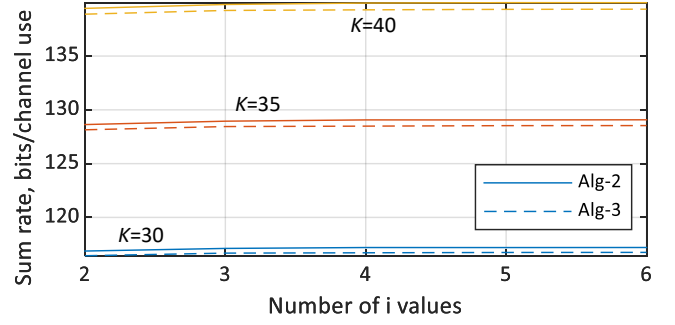


Fig. 5: Sum rate versus the number of i values used in Step 5a) of Algorithm 2, where $P = 28$ dB, and $M = 30, 35$ and 40 for the same values of K .

been illustrated in Section IV-B.

VII. CONCLUSIONS

The joint user and beam selection problem of the beamspace mmWave/THz massive MIMO downlink was studied. Motivated by its appealingly simple sum rate expression, we harnessed DPC to the joint selection problem for the first time in the open literature. We unveiled that the DPC sum rate monotonically increases with the number of selected users and it is a non-decreasing function of the number of selected beams. These features allow us to substantially simplify the user and beam selection problem. We then developed three algorithms for solving the simplified problem. The first one sequentially selects users and then beams, while the second one simultaneously selects both for reducing the extra inter-user interference encountered in the first. While the null space projection is used as a performance metric, the third algorithm further reduces the complexity by replacing the null projection by the SIR. The performance-vs-complexity analysis was carried out for the three algorithms. Our simulation results validated the efficiency of the proposed designs.

Several exciting future research problems are suggested next. First, the analysis and the proposed algorithms may be extended to user grouping and beam selection, another critical problem in beamspace massive MIMO [26]. Moreover, the applicability and extension of the proposed methods to more advanced beamspace MIMO scenarios/settings, such as wideband and phase shifters-enabled beam selection [27], [28], are worth further investigating. In addition, the proposed designs may be extended by further considering the beam selection on the user side [29]. Finally, the rate-fairness of users suffering from low SNR may be improved by relying on geometric mean rate based optimization [30].

APPENDIX

A. Proof of Lemma 2

Since \mathbf{R} is an upper triangular matrix, we have $\Pi_{u=0}^{U-1} r_u = \det \{\mathbf{R}\}$. Multiplying \mathbf{R} by an orthogonal matrix, e.g., \mathbf{Q} in (3), does not change its determinant. Thus, we have

$$\begin{aligned} \Pi_{u=0}^{U-1} r_u &= \det \{\mathbf{Q}\mathbf{R}\} = \Pi_{u=0}^{U-1} \sigma_u \\ &= \sqrt{\Pi_{u=0}^{U-1} \eta_u} = \sqrt{\det \{\mathbf{T}\}}, \end{aligned}$$

where σ_u is the u -th singular value of $(\mathbf{U}\tilde{\mathbf{H}}\mathbf{B})$, η_u is the eigenvalue of $\mathbf{\Gamma}$, and $\mathbf{\Gamma} = (\mathbf{U}\tilde{\mathbf{H}}\mathbf{B})(\mathbf{U}\tilde{\mathbf{H}}\mathbf{B})^H$. As a Hermitian matrix, $\det\{\mathbf{\Gamma}\}$ is non-decreasing with B ; so is $\prod_{u=0}^{U-1} r_u = \sqrt{\det\{\mathbf{\Gamma}\}}$.

B. Proof of Proposition 2

Assume that $m(\in [1, M-1])$ users have been selected, and their strongest beams have different indexes as collected by \mathcal{B} . Let us now consider the probability \mathcal{P} of the event \mathcal{V} : the index of the strongest beam of the next selected user is in \mathcal{B} , where \mathcal{P} is the product of the probabilities of two independent events:

- 1) The first one is that one out of $(K-m)$ remaining users is selected next. Its probability is $\mathcal{P}_1 = \frac{1}{K-m}$, since these users have equal chance of being selected.
- 2) The second event is that the selected user shares the strongest beam with any one of the m pre-selected users. Its probability is $\mathcal{P}_2 = \frac{m}{N}$, as the strongest beam of each user can be one of the N beams with the same probability.

Using the two probabilities, we obtain $\mathcal{P} = \mathcal{P}_1\mathcal{P}_2 = \frac{m}{(K-m)N}$.

Given K users and the probability \mathcal{P} , $K\mathcal{P} < 1$ implies that less than one, out of $(K-m)$ remaining users, will share the strongest beam with one of the m selected users; in other words, the event \mathcal{V} almost never happens. Solving the following problem leads to the upper limit of m :

$$\bar{M} = \lfloor m^* \rfloor, \text{ s.t. } \frac{m^*K}{(K-m^*)N} = 1, \quad (31)$$

where $\lfloor \cdot \rfloor$ rounds the enclosed number towards negative infinity. Provided that $\bar{M} \geq M$ (the number of RF chains), we can state almost for sure that \mathcal{V} cannot happen, or otherwise the event \mathcal{E} given in the statement of Proposition 2 always happens.

REFERENCES

- [1] W. Saad, M. Bennis, and M. Chen, "A vision of 6G wireless systems: Applications, trends, technologies, and open research problems," *IEEE Network*, vol. 34, no. 3, pp. 134–142, 2020.
- [2] X. You, C.-X. Wang, J. Huang, X. Gao, Z. Zhang, M. Wang, Y. Huang, C. Zhang, Y. Jiang, J. Wang *et al.*, "Towards 6G wireless communication networks: Vision, enabling technologies, and new paradigm shifts," *Science China Information Sciences*, vol. 64, no. 1, pp. 1–74, 2021.
- [3] L. Bariah, L. Mohjazi, S. Muhaidat, P. C. Sofotasios, G. K. Kurt, H. Yanikomeroglu, and O. A. Dobre, "A prospective look: Key enabling technologies, applications and open research topics in 6G networks," *IEEE Access*, vol. 8, pp. 174 792–174 820, 2020.
- [4] I. A. Hemadeh, K. Satyanarayana, M. El-Hajjar, and L. Hanzo, "Millimeter-wave communications: Physical channel models, design considerations, antenna constructions, and link-budget," *IEEE Commun. Surv. Tutor.*, vol. 20, no. 2, pp. 870–913, 2018.
- [5] X. Gao, L. Dai, and A. M. Sayeed, "Low RF-complexity technologies to enable millimeter-wave MIMO with large antenna array for 5G wireless communications," *IEEE Commun. Mag.*, vol. 56, no. 4, pp. 211–217, 2018.
- [6] K. Wu, W. Ni, T. Su, R. P. Liu, and Y. J. Guo, "Efficient Angle-of-Arrival estimation of lens antenna arrays for wireless information and power transfer," *IEEE J. Sel. Areas Commun.*, vol. 37, no. 1, pp. 116–130, Jan 2019.
- [7] Y. Zeng and R. Zhang, "Millimeter wave MIMO with lens antenna array: A new path division multiplexing paradigm," *IEEE Trans. Commun.*, vol. 64, no. 4, pp. 1557–1571, 2016.
- [8] Y. J. Guo, M. Ansari, and N. J. G. Fonseca, "Circuit type multiple beamforming networks for antenna arrays in 5G and 6G terrestrial and non-terrestrial networks," *IEEE J. Microw.*, vol. 1, no. 3, pp. 704–722, 2021.
- [9] Y. J. Guo, M. Ansari, R. W. Ziolkowski, and N. J. G. Fonseca, "Quasi-optical multi-beam antenna technologies for B5G and 6G mmwave and THz networks: A review," *IEEE Open J. Antennas Propag.*, vol. 2, pp. 807–830, 2021.
- [10] A. Sayeed and J. Brady, "Beamspace MIMO for high-dimensional multiuser communication at millimeter-wave frequencies," in *2013 IEEE GLOBECOM*. IEEE, 2013, pp. 3679–3684.
- [11] R. Guo, Y. Cai, M. Zhao, Q. Shi, B. Champagne, and L. Hanzo, "Joint design of beam selection and precoding matrices for mmwave MU-MIMO systems relying on lens antenna arrays," *IEEE J. Sel. Top. Signal Process.*, vol. 12, no. 2, pp. 313–325, 2018.
- [12] X. Gao, L. Dai, S. Zhou, A. M. Sayeed, and L. Hanzo, "Wideband beamspace channel estimation for millimeter-wave MIMO systems relying on lens antenna arrays," *IEEE Trans. Signal Process.*, vol. 67, no. 18, pp. 4809–4824, 2019.
- [13] J. Yang, C.-K. Wen, S. Jin, and F. Gao, "Beamspace channel estimation in mmwave systems via cosparse image reconstruction technique," *IEEE Trans. Commun.*, vol. 66, no. 10, pp. 4767–4782, 2018.
- [14] X. Gao, L. Dai, Z. Chen, Z. Wang, and Z. Zhang, "Near-optimal beam selection for beamspace mmwave massive MIMO systems," *IEEE Commun. Lett.*, vol. 20, no. 5, pp. 1054–1057, 2016.
- [15] P. V. Amadori and C. Masouros, "Low RF-complexity millimeter-wave beamspace-MIMO systems by beam selection," *IEEE Trans. Commun.*, vol. 63, no. 6, pp. 2212–2223, 2015.
- [16] H. Yu, W. Qu, Y. Fu, C. Jiang, and Y. Zhao, "A novel two-stage beam selection algorithm in mmwave hybrid beamforming system," *IEEE Commun. Lett.*, vol. 23, no. 6, pp. 1089–1092, 2019.
- [17] R. Pal, K. V. Srinivas, and A. K. Chaitanya, "A beam selection algorithm for millimeter-wave multi-user MIMO systems," *IEEE Commun. Lett.*, vol. 22, no. 4, pp. 852–855, 2018.
- [18] Q. Zhang, X. Li, B.-Y. Wu, L. Cheng, and Y. Gao, "On the complexity reduction of beam selection algorithms for beamspace MIMO systems," *IEEE Wireless Commun. Lett.*, vol. 10, no. 7, pp. 1439–1443, 2021.
- [19] Z. Cheng, Z. Wei, and H. Yang, "Low-complexity joint user and beam selection for beamspace mmwave MIMO systems," *IEEE Commun. Lett.*, vol. 24, no. 9, pp. 2065–2069, 2020.
- [20] S. Ahmadi, *5G NR: Architecture, Technology, Implementation, and Operation of 3GPP New Radio Standards*. Academic Press, 2019.
- [21] K. Wu, W. Ni, T. Su, R. P. Liu, and Y. J. Guo, "Expedition estimation of angle-of-arrival for hybrid butler matrix arrays," *IEEE Trans. Wireless Commun.*, vol. 18, no. 4, pp. 2170–2185, April 2019.
- [22] X. Gao, L. Dai, S. Han, C.-L. I, and X. Wang, "Reliable beamspace channel estimation for millimeter-wave massive MIMO systems with lens antenna array," *IEEE Trans. Wireless Commun.*, vol. 16, no. 9, pp. 6010–6021, 2017.
- [23] X. Gao, L. Dai, Y. Zhang, T. Xie, X. Dai, and Z. Wang, "Fast channel tracking for thz beamspace massive MIMO systems," *IEEE Trans. Vehic. Techn.*, vol. 66, no. 7, pp. 5689–5696, 2016.
- [24] Y. S. Cho, J. Kim, W. Y. Yang, and C. G. Kang, *MIMO-OFDM wireless communications with MATLAB*. John Wiley & Sons, 2010.
- [25] G. Dimic and N. Sidiropoulos, "On downlink beamforming with greedy user selection: performance analysis and a simple new algorithm," *IEEE Trans. Signal Process.*, vol. 53, no. 10, pp. 3857–3868, 2005.
- [26] J. Sun, M. Jia, Q. Guo, and X. Gu, "Joint user grouping and beam selection for beamspace mmwave multi-user MIMO system," *IEEE Commun. Lett.*, vol. 26, no. 5, pp. 1170–1174, 2022.
- [27] W. Shen, X. Bu, X. Gao, C. Xing, and L. Hanzo, "Beamspace precoding and beam selection for wideband millimeter-wave MIMO relying on lens antenna arrays," *IEEE Trans. Signal Process.*, vol. 67, no. 24, pp. 6301–6313, 2019.
- [28] Z. Cheng, Z. Wei, H. Li, and H. Yang, "SLNR-based beamspace precoding and beam selection for wideband mmwave massive MIMO," *IEEE Commun. Lett.*, vol. 26, no. 2, pp. 478–482, 2022.
- [29] J. Choi, "Beam selection in mm-wave multiuser MIMO systems using compressive sensing," *IEEE Trans. Commun.*, vol. 63, no. 8, pp. 2936–2947, 2015.
- [30] H. Yu, H. D. Tuan, E. Dutkiewicz, H. V. Poor, and L. Hanzo, "Maximizing the geometric mean of user-rates to improve rate-fairness: Proper vs. improper gaussian signaling," *IEEE Trans. Wirel. Commun.*, vol. 21, no. 1, pp. 295–309, 2022.